Molecular Cell, Vol. 12, 87–100, July, 2003, Copyright ©2003 by Cell Press

# The CCT Chaperonin Promotes Activation of the Anaphase-Promoting Complex through the Generation of Functional Cdc20

**Alain Camasses, Aliona Bogdanova, Andrej Shevchenko, and Wolfgang Zachariae***
Max Planck Institute of Molecular Cell Biology and Genetics
Pfotenhauerstrasse 108
01307 Dresden
Germany

## Summary

**The WD repeat protein Cdc20 is essential for progression through mitosis because it is required to activate ubiquitin ligation by the anaphase-promoting complex (APC/C). Here we show in yeast that Cdc20 binds to the CCT chaperonin, which is known as a folding machine for actin and tubulin. The CCT is required for Cdc20's ability to bind and activate the APC/C. In vivo, CCT is essential for Cdc20-dependent cell cycle events such as sister chromatid separation and exit from mitosis. The chaperonin is also required for the function of the Cdc20-related protein Cdh1, which activates the APC/C during G1. We propose that folding of the Cdc20 family of APC/C activators is an essential and evolutionary conserved function of the CCT chaperonin.**

## Introduction

Progression through mitosis depends on the proteolysis of cell cycle regulators by the ubiquitin-proteasome pathway. Degradation of Pds1/securin causes entry into anaphase through activation of the protease Esp1/separase, which destroys the cohesion between sister sequences and enables the mitotic spindle to pull sister chromatids to opposite poles of the cell (Nasmyth et al., 2000). Exit from mitosis and cytokinesis requires inactivation of the Cdk1-cyclin B kinase, which involves proteolysis of the cyclin B subunit (Glotzer et al., 1991). Additional proteins are degraded during anaphase including mitotic kinases and regulators of spindle function.

Mitotic degradation of cell cycle regulators is triggered by the anaphase-promoting complex or cyclosome (APC/C), an ubiquitin ligase consisting of at least 11 evolutionary conserved subunits (Zachariae and Nasmyth, 1999). The APC/C is only active as a ligase after binding to either Cdc20 or Cdh1/Hct1. Both proteins contain WD repeats in their C termini, which are thought to fold into a seven-bladed β propeller (Smith et al., 1999). Cdc20 and Cdh1 specifically recognize APC/C substrates, suggesting that they activate ubiquitination by recruiting substrates to the ligase particle (Vodermaier, 2001). The WD proteins mediate the temporal control of APC/C-dependent proteolysis, which commences shortly before the onset of anaphase and persists until late G1 of the subsequent cell cycle. Activation of the APC/C by Cdc20 at the metaphase-to-anaphase transition is essential for sister chromatid separation and to initiate the destruction of cyclin-dependent kinases (CDKs). During late anaphase, Cdc20 is replaced by Cdh1, which sustains APC/C activity during exit from mitosis and G1. During other cell cycle stages, Cdh1 is phosphorylated by CDKs, which blocks association with the APC/C.

Several mechanisms have been implicated in controlling the formation and activation of the APC/C-Cd20 holoenzyme (Peters, 2002). In yeast and mammalian cells, Cdc20 is only present during G2 and mitosis due to cell cycle-regulated transcription and APC/C-dependent proteolysis. However, there is a lag period between the appearance of Cdc20 in G2 and its binding to the APC/C in metaphase. Binding of Cdc20 might be facilitated by the phosphorylation of APC/C subunits during mitosis, but it is unclear whether this modification is essential for the activation of APC/C-Cdc20. Activation of APC/C-Cdc20 is blocked by the spindle assembly checkpoint as long as sister kinetochores are present that have failed to attach to microtubules emanating from opposite spindle poles (Musacchio and Hardwick, 2002). The binding to Cdc20 of checkpoint proteins such as Mad2 is essential for checkpoint function, but how they inhibit APC/C-Cdc20 is unknown.

In a search for proteins associated with Cdc20, we identified a 900 kDa complex called the chaperonin-containing TCP1 or CCT (also called TRiC for TCP1 containing ring complex) (Gutsche et al., 1999). CCT is composed of eight evolutionary conserved subunits, which are arranged into two octameric rings that form a cylindrical complex. The chaperonin encapsulates nonnative proteins in the central cavity and promotes their folding in an ATP-dependent reaction. Initially, only actin and tubulin have been described as natural substrates of the CCT, suggesting a specific role for this chaperonin in maintaining the integrity of the cytoskeleton (Sternlicht et al., 1993). Accordingly, mutations in budding yeast *CCT* genes cause defects in actin- and tubulin-dependent structures (Stoldt et al., 1996). Recent work, however, has identified several noncytoskeletal proteins that require CCT for proper folding, suggesting that CCT's substrate spectrum is broader than originally proposed (Dunn et al., 2001). Here we demonstrate that the CCT from budding yeast has an essential function in cell cycle progression, which is to promote activation of the APC/C through the generation of active Cdc20 and Cdh1.

## Results

### Specific Association of Cdc20 with the CCT Chaperonin

To estimate the fraction of Cdc20 that was associated with the APC/C, we separated in glycerol density gradients extracts from yeast cells containing epitope-tagged versions of Cdc20 and the APC/C component Cdc16 (Figure 1A). Most of Myc18-Cdc20 migrated between 10S and 22S, and only a small fraction cosedimented

*Correspondence: zachariae@mpi-cbg.de

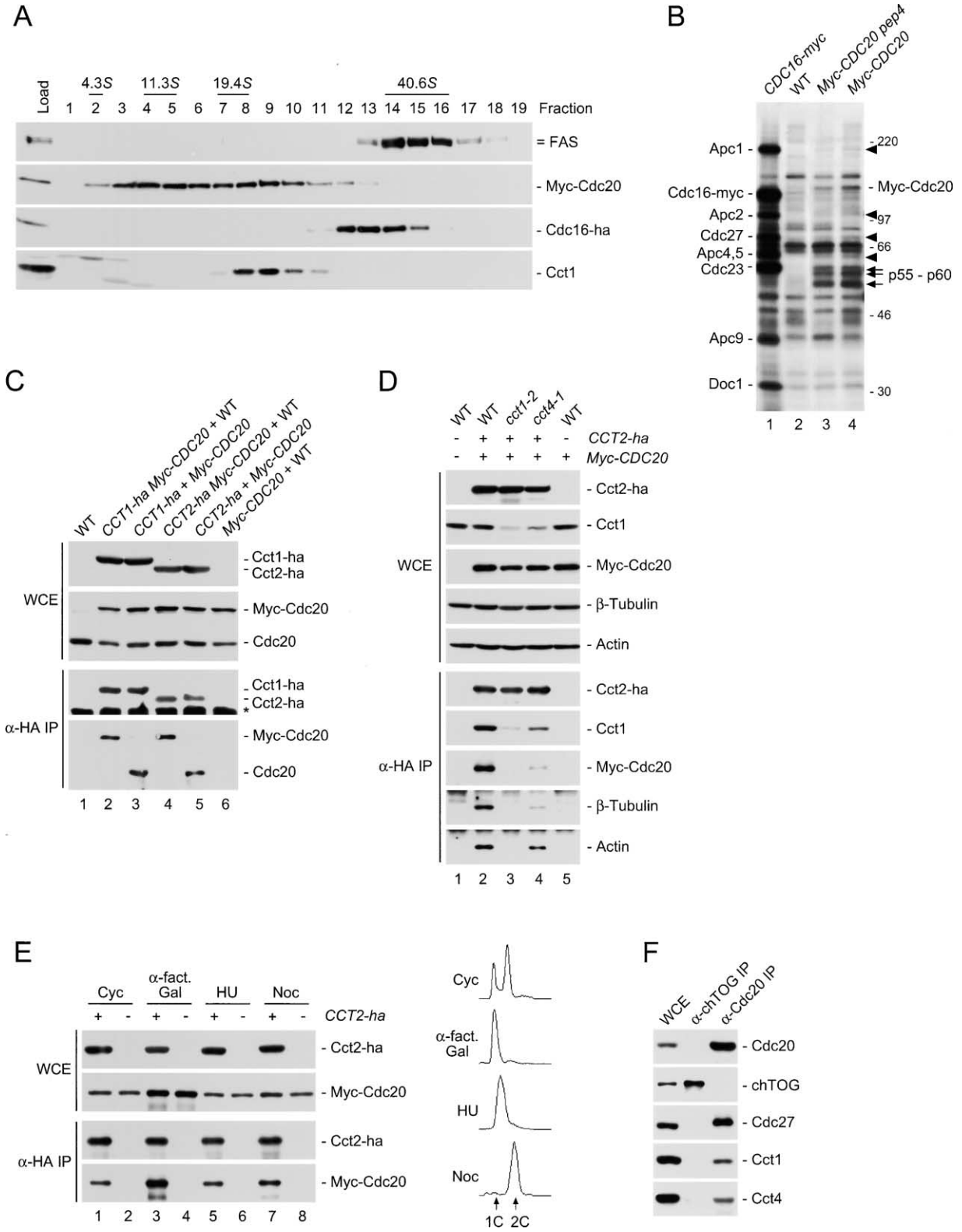


Figure 1. Specific Binding of Cdc20 to the CCT

(A) Glycerol density gradient centrifugation of an extract from *Myc18-CDC20 CDC16-ha3* cells (Z425). Fractions were analyzed by immunoblotting. FAS, fatty acid synthetase (40.6S). BSA (4.3S), catalase (11.3S), and thyroglobulin (19.4S) were separated in parallel.

(B) Separation of anti-Myc immunoprecipitates from $^{35}$S-labeled wild-type (WT, Z1885), *CDC16-myc6* (Z153), *Myc18-CDC20* (Z1899), and *Myc18-CDC20 pep4*Δ (Z419) cells. Arrows, CCT subunits; arrowheads, APC/C components.

(C) Immunoblot analysis of anti-HA immunoprecipitates prepared after mixing two strains with the indicated genotypes. The asterisk labels antibody bands. Strains: 1, Z651; 2, Z991 + Z651; 3, Z960 + Z1009; 4, Z989 + Z651; 5, Z910 + Z1009; 6, Z1009 + Z651.

with the APC/C particle at 36S, suggesting that a large fraction of Cdc20 was associated with other complexes. To identify Cdc20 binding proteins, we compared immunoprecipitates from *Myc18-CDC20* and *CDC16-myc6* cells labeled with $^{35}$S. Myc18-Cdc20 samples contained weak signals from APC/C components (Figure 1B, arrowheads) and several bands of 55–60 kDa (Figure 1B, arrows). Similar bands were detected by silver staining in gels loaded with preparative Myc18-Cdc20 immunoprecipitates (data not shown). Mass spectrometric analysis identified the proteins Cct1/Tcp1, Cct3, Cct4, Cct5, Cct6, and Cct8, which are all subunits of the CCT chaperonin. Accordingly, the high molecular weight forms of Cdc20 comigrated with the CCT at 20S through the glycerol gradient (Figure 1A).

The genes *CCT1* and *CCT2* were modified to encode functional, HA3-tagged proteins (see Experimental Procedures). Anti-HA immunoprecipitations revealed that both Myc9-Cdc20 and the untagged protein bound to the CCT with similar efficiency (data not shown but similar to Figure 1C). The stable interaction between CCT and Cdc20 was specific since no interaction of Cct2-ha3 could be detected with Myc9-Cdc5, Myc9-Cdc15, and 22 untagged proteins ranging in size from 18 to 126 kDa (data not shown, see Experimental Procedures). Notably, CCT immunoprecipitates did not contain APC/C components, suggesting that CCT binds to Cdc20 by itself but not to the APC/C-Cdc20 holoenzyme. In summary, our data imply that Cdc20, together with actin and tubulin, belongs to a restricted set of proteins that specifically bind to the CCT with high affinity.

We next investigated whether the interaction between Cdc20 and the CCT occurred in vivo or after cell lysis in the extract. A mixing experiment was performed to test whether the Cdc20-CCT complex could form de novo in the extract (Figure 1C). Equal amounts of *CCT1-ha3 Myc9-CDC20* cells and wild-type cells were mixed and then lysed. Analysis of anti-HA immunoprecipitates with antibodies to Cdc20 revealed that Myc9-Cdc20 but not Cdc20 was bound to Cct1-ha3 in this extract (Figure 1C, lane 2). In contrast, Cdc20, but not Myc9-Cdc20, was associated with Cct1-ha3 after mixing *CCT1-ha3* cells with *Myc9-CDC20* cells (lane 3). Similar results were obtained with *CCT2-ha3* strains (lanes 4 and 5). It was always the endogenous Cdc20 protein that bound to the tagged CCT subunits, demonstrating that Cdc20 was unable to bind de novo to the CCT in our extracts. Thus, coimmunoprecipitation reflects an interaction established in vivo.

To test whether binding of Cdc20 to CCT subunits required the integrity of the chaperonin, we introduced into a *CCT2-ha3 Myc18-CDC20* strain the temperature-sensitive (ts) mutations *cct1-2/tcp1-2* and *cct4-1/anc2-1*, which cause defects in the cytoskeleton at 37°C (Ursic et al., 1994; Vinh and Drubin, 1994). Anti-HA immunoprecipitations from strains shifted to 37°C revealed reduced amounts of Cct1 in *cct1-2* mutant cells generating a structurally defective CCT (Figure 1D). The *cct1-2* mutation abolished the interaction of Cct2-ha3 with actin and tubulin whereas *cct4-1* reduced the interaction with tubulin but had little effect on the binding of actin. Coimmunoprecipitation of Myc9-Cdc20 with Cct2-ha3 was undetectable in the *cct1-2* mutant and severely reduced in the *cct4-1* mutant. These data show that association of Cdc20 with the CCT requires a functional chaperonin. In contrast, the activity of APC/C-Cdc20 was not required for Cdc20's ability to bind to the CCT. *cdc20-1* and *cdc20-3* mutant cells fail to activate the APC/C and arrest in metaphase at 37°C. Nevertheless, the mutant Cdc20 proteins still bound efficiently to the CCT. Cdc20 also associated normally with the CCT in cells containing ts mutations in APC/C components (data not shown).

We also investigated whether the CCT-Cdc20 interaction was regulated during the cell cycle (Figure 1E). Myc18-Cdc20 was associated with Cct2-ha3 in proliferating cells and in cells arrested in S phase or in mitosis. Cdc20 is not expressed during G1. However, expression of Myc18-Cdc20 from the *GAL1* promoter in $\alpha$ factor-arrested *CCT2-ha3* cells showed that Cdc20 could also bind to the CCT during G1 (Figure 1E, lanes 3 and 4). These data suggest that the CCT can recognize Cdc20 throughout the cell cycle. Association of Cdc20 with CCT subunits was also observed in extracts from human cells (Figure 1F), suggesting that binding to the CCT is an evolutionary conserved feature of Cdc20.

### Release of Cdc20 from the CCT Depends on the Hydrolysis of ATP

Hydrolysis of ATP is required for the release of folded actin and tubulin from the CCT (Gutsche et al., 1999). To test whether the CCT-Cdc20 interaction was sensitive to ATP, anti-HA immunoprecipitates were prepared from *CCT1-ha3 Myc9-CDC20* cells and washed extensively. Addition of ATP but not buffer alone caused a time-dependent release of Myc9-Cdc20, actin, and tubulin from the immobilized chaperonin into the supernatant (Figure 2A). Similar results were obtained when the CCT was immunoprecipitated from *CCT2-ha3* strains (data not shown). As shown in Figure 2B, release of Myc9-Cdc20, actin, and tubulin occurred in the presence of ATP but not in the presence of the nonhydrolyzable analogs ATP-$\gamma$S and AMP-PNP. We conclude that Cdc20 behaves similar to actin and tubulin in that it is released from the CCT in a reaction driven by the hydrolysis of ATP. This finding supports the notion that Cdc20 is a substrate of the CCT.

(D) Immunoblot analysis of anti-HA immunoprecipitates from *Myc9-CDC20 CCT2-ha3* strains containing *cct* mutations. Strains were grown at 25°C and shifted to 37°C for 90 min. Strains: 1, Z651; 2, Z989; 3, Z1420; 4, Z1416; 5, Z1009.

(E) *Myc18-CDC20 CCT2-ha3* (+, Z958) and *Myc18-CDC20* (−, Z446) strains were arrested at 30°C with hydroxyurea (HU) and nocodazole (Noc), or left untreated (Cyc). In the $\alpha$ factor-arrested cells (lane 3, Z1937; lane 4, Z921), Myc18-Cdc20 was expressed from the *GAL1* promoter for 90 min. Left panel, immunoblot analysis of anti-HA immunoprecipitates. Right panel, cellular DNA content of the *CCT2-ha3* strains.

(F) Immunoblot analysis of anti-Cdc20 and anti-chTOG (a microtubule binding protein used as control) immunoprecipitates from HeLa cells.

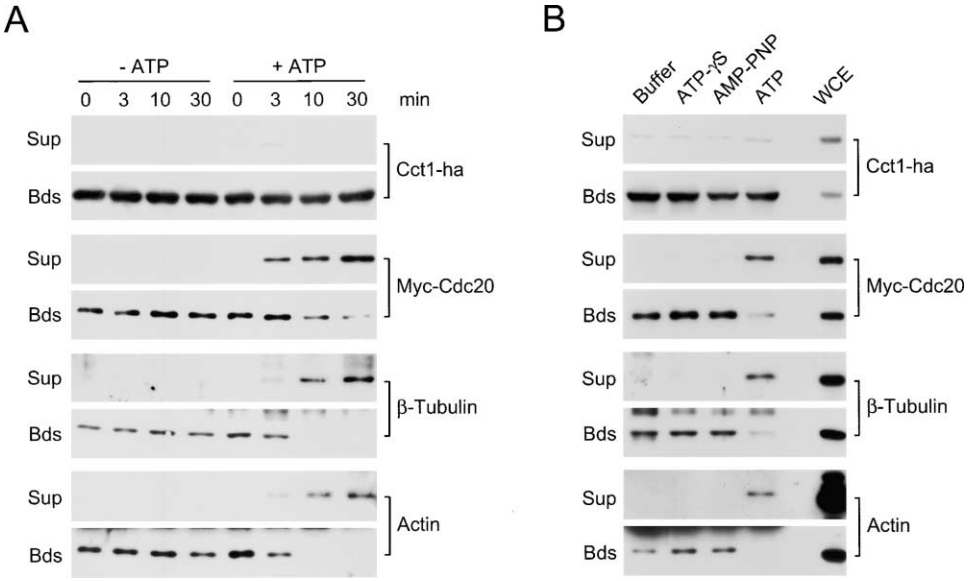


Figure 2. ATP-Dependent Release of Cdc20 from the CCT

(A) Anti-HA immunoprecipitates prepared from *CCT1-ha3 Myc9-CDC20 pep4*Δ cells (Z1411) were incubated at 25°C with buffer containing or lacking Mg/ATP. At different time points, reactions were stopped with EDTA and separated into supernatant (Sup) and beads (Bds) fractions, which were analyzed by immunoblotting.

(B) The immunoprecipitates were incubated for 20 min with buffer, Mg/ATP, or the nonhydrolyzable analogs Mg/ATP-γS and Mg/AMP-PNP. Reactions were analyzed as in (A). 10 μg of extract (WCE) was analyzed in all panels.

## CCT Is Required for Binding of Cdc20 to the APC/C and to Checkpoint Proteins

We investigated whether the CCT was required for Cdc20's ability to bind to the APC/C. *Myc18-CDC20* strains containing different *cct* mutations were shifted to 37°C followed by immunoprecipitations of Apc2 (Figure 3A). Myc18-Cdc20 bound to Apc2 in wild-type extracts, but this interaction was undetectable in extracts from *cct1-2* cells and severely reduced in extracts from *cct2-326* and *cct4-1* cells. In contrast, the APC/C components Cdc23 and Cdc27 were associated with Apc2 in all the extracts. The *cct1-2* mutation was used in further experiments because it caused the strongest defect in binding of Cdc20 to the CCT and the APC/C. At 37°C, cell cycle progression was defective in *cct1-2* mutants (see below). To control for potential cell cycle effects, association of Cdc20 with the APC/C was analyzed in wild-type and *cct1-2* mutant cells arrested at 25°C in S phase or in mitosis and then shifted to 37°C. Under all conditions, binding of Myc18-Cdc20 to the APC/C component Cdc23-ha3 was strongly reduced in *cct1-2* cells, whereas binding of two other APC/C components, Apc2 and Cdc16, was normal (Figure 3B). These data show that the CCT is required for the binding of Cdc20 to the APC/C, but not for some of the protein-protein interactions within the APC/C particle.

We next considered whether defects in the cytoskeleton rather than defects in the CCT per se prevented the binding of Cdc20 to the APC/C in *cct* mutants. Neither the microtubule-depolymerizing drug nocodazole (Figure 3B) nor the actin-depolymerising drug latrunculin B (Figure 3C) reduced the ability of Myc18-Cdc20 to associate with Cdc23-ha3. This suggests that maintaining the integrity of the cytoskeleton and promoting the formation of the APC/C-Cdc20 holoenzyme are independent functions of the CCT.

A mixing experiment was performed to test whether the CCT is required by Cdc20 or by the APC/C to form the APC/C-Cdc20 holoenzyme (Figure 3D). A *CDC23-ha3* strain and a *Myc18-CDC20* strain were grown at 25°C and shifted to 37°C for 120 min. Equal amounts of cells from both strains were mixed and then lysed. Analysis of anti-HA immunoprecipitates with an antibody to Cdc20 revealed that both Cdc20 and Myc18-Cdc20 associated with Cdc23-ha3 in this extract, demonstrating that the APC/C-Cdc20 complex was formed de novo in the extract (Figure 3D, lane 2). Myc18-Cdc20, but not Cdc20, bound to Cdc23-ha3 after mixing *Myc18-CDC20* cells with *CDC23-ha3 cct1-2* mutant cells (lane 3). In contrast, Cdc20, but not Myc18-Cdc20, bound to Cdc23-ha3 after mixing *CDC23-ha3* cells with *Myc18-CDC20 cct1-2* mutant cells (lane 4). In summary, it was always the Cdc20 protein (tagged or untagged) from the *CCT1* wild-type cells that bound to Cdc23-ha3. We conclude that Cdc20, but not the APC/C, requires the activity of the CCT for the formation of the APC/C-Cdc20 complex.

We also tested whether CCT was required for the interaction of Cdc20 with components of the spindle assembly checkpoint. Mad2 was associated with Myc9-Cdc20 in wild-type but not in *cct1-2* extracts (Figure 3E, lanes 3 and 4). Mad2 was functional in *cct1-2* cells because it still bound to Mad1-myc9 (Figure 3E, lanes 5 and 6), whose Mad2 binding site is similar to that of Cdc20 (Luo et al., 2002; Sironi et al., 2002). Also, the checkpoint protein Bub3-ha3 was bound to Myc18-Cdc20 in wild-type but not in *cct1-2* mutant extracts (Figure 3F, lanes 5 and 6). Bub3 contains, like Cdc20,

seven WD repeats, raising the possibility that Bub3 function also required CCT activity. This was unlikely, however, because Bub3-ha3 was associated with the protein kinase Bub1-myc18 in extracts from wild-type and *cct1-2* mutant cells shifted to 37°C (Figure 3F, lanes 2 and 3). Accordingly, no interaction could be detected between Bub3 and the CCT (data not shown). In summary, our data show that CCT is required for Cdc20's ability to interact with the APC/C and checkpoint proteins.

### Analysis of CCT Function In Vivo

To analyze whether CCT is required for Cdc20 function in vivo, we first defined the cell cycle events that do and those that do not depend on the chaperonin. Small G1 cells were isolated by centrifugal elutriation from a wild-type and a *cct1-2* strain and released into a synchronous cell cycle at 37°C. The mean volume of *cct1-2* cells increased with the same kinetics as that of wild-type cells, suggesting that cellular growth was largely normal (Figure 4A). Accordingly, *cct1-2* cells synthesized Cdc20, the microtubule motor Kip1, and the mitotic cyclin Clb2 (Figure 4C). Expression of these proteins is induced during G2 and mitosis in wild-type cells and requires Cdk1 kinase activity (Amon et al., 1993; Gordon and Roof, 2001; Prinz et al., 1998). Elutriation of *cct1-2 Myc18-CDC20* cells showed that Cdc20 was still imported into the nucleus at 37°C (data not shown). The mutant cells also degraded the CDK inhibitor Sic1 and then replicated their DNA (Figures 4B and 4C).

Budding was delayed or even failed in many *cct1-2* cells (Figure 4A). In cells that managed to produce a bud, cellular growth was directed more to the mother cells than to the bud. This defect in polarized growth was correlated with defects in the actin cytoskeleton (data not shown). Actin patches were slow or even failed to accumulate at the presumptive bud site. Also in small-budded cells the distribution of actin patches appeared less polarized than in wild-type cells. Anti-tubulin immunofluorescence revealed that the astral microtubules initially present in small G1 cells deteriorated over time and that mitotic spindles failed to form (data not shown). Accordingly, nuclear division was undetectable. The mutant cells failed to initiate the APC/C-dependent proteolysis of Clb2, Kip1, and Cdc20, they failed to undergo cytokinesis, and they failed to rereplicate their DNA (Figures 4A–4C). The cytoskeletal defects observed in *cct1-2* cells are consistent with the failure of the mutant CCT complex to bind to actin and tubulin. Significantly, several processes including cellular growth and DNA replication did occur in the mutant cells.

The failure of *cct1-2* mutants to degrade APC/C substrates could result from the inhibition of APC/C-Cdc20 by the spindle assembly checkpoint or from a nonfunctional Cdc20. High levels of Cdc20 were shown to induce degradation of Pds1 even under conditions that would stabilize Pds1 in normal cells, such as activation of the spindle assembly checkpoint (Shirayama et al., 1998; Visintin et al., 1997). To test whether the CCT was directly required for the proteolysis of Pds1, Cdc20 was overexpressed from the inducible *MET25* promoter at 37°C in wild-type and *cct1-2* mutant cells. High levels of Cdc20 lead to the rapid degradation of Pds1-myc18 in wild-type cells, but not in *cct1-2* mutant cells (Figure 4D). To control for potential cell cycle effects, the experiment was repeated with cells arrested in S phase. Again, high levels of Cdc20 induced the degradation of Pds1-myc18 in wild-type, but not in the mutant cells (Figure 4E). These data show that activation of APC/C-dependent proteolysis by Cdc20 requires CCT function.

### CCT Is Required for Sister Chromatid Separation and Exit from Mitosis

The finding that Cdc20 activity requires CCT in vivo predicts that CCT should be required for the same cell cycle events as Cdc20. To test this prediction, we followed Pds1 protein levels, the behavior of sister chromatids, and cytokinesis as wild-type and *cct1-2* mutant cells synchronously progressed through mitosis. To observe sister sequences, the *URA3* locus on chromosome V was marked with GFP (Michaelis et al., 1997). From G1 until metaphase, cells show a single GFP dot, which splits into two when sister chromatids separate. Since budding is delayed in *cct1-2* strains, cells were arrested at 25°C with hydroxyurea, which blocks DNA replication but not budding. The arrested cells were shifted to 37°C to inactivate the CCT, washed, and released at 37°C into medium lacking hydroxyurea and containing $\alpha$ factor. The pheromone was added to arrest in G1 those cells that managed to exit from mitosis. Upon release, wild-type cells replicated their DNA within 30 min, degraded Pds1 and separated sister chromatids between 30 and 60 min, and then destroyed the Clb2 cyclin. Cells accumulated Sic1 as they underwent cytokinesis and arrested in G1 (Figure 5A). Also *cct1-2* mutant cells replicated their DNA within 30 min after release but then failed to degrade Pds1, to separate sister chromatids, and to exit from mitosis (Figure 5B). Inactivation of the spindle assembly checkpoint by deletion of the *MAD2* gene failed to cause Pds1 degradation and sister chromatid separation in *cct1-2* cells (Figure 5C). Similar results were obtained after deleting the *SWE1* gene in *cct1-2 mad2*$\Delta$ cells (Figure 5D). Swe1 is required for the morphogenesis checkpoint, which is activated by defects in the actin cytoskeleton and blocks nuclear division (Lew, 2000). We conclude that the CCT has an essential role in Pds1 degradation and sister chromatid separation that is independent from its function in the folding of actin and tubulin. The DNA damage checkpoint, which depends on the *RAD9* gene, was shown to block sister chromatid separation by inhibiting the degradation of Pds1 (Wang et al., 2001). However, *cct1-2 mad2*$\Delta$ *swe1*$\Delta$ *rad9*$\Delta$ quadruple mutants failed to degrade Pds1 and to separate sisters (Figure 5E). In summary, these data support the idea that the CCT is essential for sister chromatid separation because it is required for the activity of Cdc20.

Deletion of *PDS1* causes sister chromatid separation in *apc* and *cdc20* mutants, demonstrating that APC/C-Cdc20's sole essential role in sister separation is to promote degradation of Pds1 (Ciosk et al., 1998). Figure 5F shows that deletion of *PDS1* caused *cct1-2* mutant cells to efficiently separate their sister chromatids although the Cdc20 substrate Kip1 remained stable. We conclude that CCT's sole essential role in sister separation is to promote the degradation of Pds1 through APC/

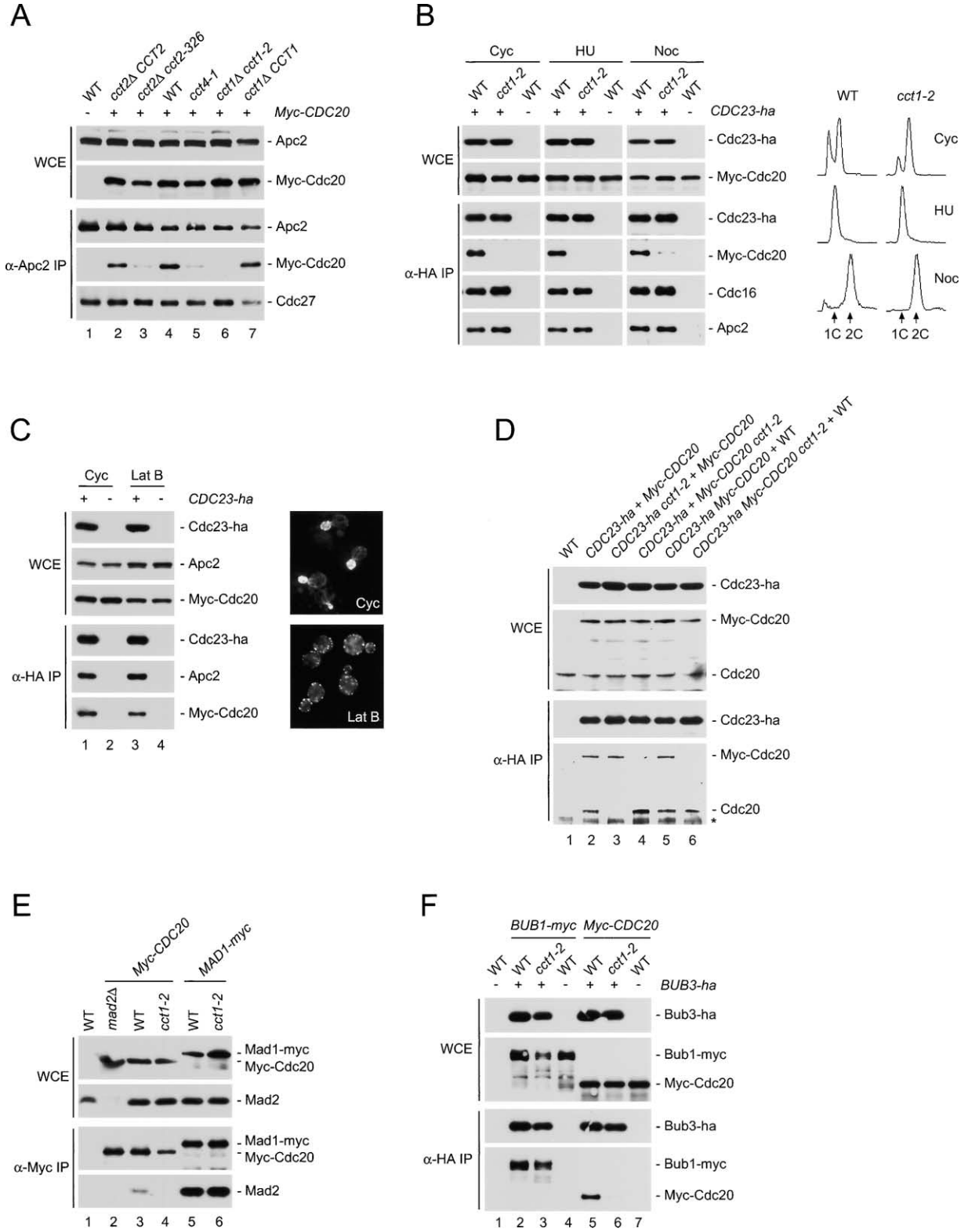


Figure 3. CCT Is Required for Cdc20's Ability to Bind to the APC/C and to Checkpoint Proteins

(A) Immunoprecipitation of Apc2 from *CDC20* (−) and *Myc18-CDC20* (+) strains containing different *cct* mutations grown at 25°C and shifted to 37°C for 90 min. Strains: 1, Z898; 2, Z1342; 3, Z1343; 4, Z1287; 5, Z1346; 6, Z1088; 7, Z1109.

(B) *Myc18-CDC20 CDC23-ha3* (Z1113), *Myc18-CDC20 CDC23-ha3 cct1-2* (Z1090), and *Myc18-CDC20* (Z446) cells were grown at 25°C (Cyc) and arrested with hydroxyurea (HU) or nocodazole (Noc) and then shifted to 37°C for 120 min. Left panel, immunoblot analysis of anti-HA immunoprecipitates. Right panel, cellular DNA content of *Myc18-CDC20 CDC23-ha3* wild-type and *cct1-2* strains.

C-Cdc20. Most *cct1-2 pds1*Δ double mutant cells failed to segregate sister chromatids all the way to opposite poles of the cells because sister segregation (but not separation) requires a functional spindle. The spindles generated during the arrest at 25°C were stable in Pds1-containing *cct1-2* mutants but deteriorated rapidly as *cct1-2 pds1*Δ cells initiated spindle elongation.

Similar to *apc pds1*Δ and *cdc20 pds1*Δ mutants, *cct1-2 pds1*Δ cells failed to exit from mitosis. This transition requires the Cdc20-mediated degradation of Pds1 and B-type cyclins and is blocked by the *BUB2*-dependent spindle-positioning checkpoint until the spindle has been inserted into the bud neck (Burke, 2000). In *cct1-2 pds1*Δ mutants, we frequently observed two GFP dots (i.e., separated sisters) in one cell body of large budded cells, indicating defects in nuclear positioning and spindle orientation. However, degradation of Clb2 and accumulation of Sic1 were still blocked in *cct1-2 pds1*Δ *bub2*Δ triple mutant cells, demonstrating that the spindle-positioning checkpoint is not essential for blocking mitotic exit in *cct1-2 pds1*Δ cells (Figure 5G). Taken together, our data demonstrate that the CCT is required for the function of APC/C-Cdc20 during entry into and exit from anaphase.

### CCT Binds to the WD Repeat Domain of Cdc20

Next, we defined the region of Cdc20 recognized by the CCT. The primary sequence of Cdc20 can be divided into three regions: an N-terminal region containing the Mad2 binding site followed by seven WD repeats and a short C-terminal region (Figure 6A). Cdc20 fragments carrying Myc18 tags at their N termini were expressed from the *GAL1* promoter in *CCT2-ha3* strains followed by anti-HA immunoprecipitations (Figure 6B). Deletion of the N-terminal (lane 5) or the C-terminal region (lane 2) did not significantly reduce binding of the remaining fragments to Cct2-ha3. Accordingly, the N-terminal region did not interact with the CCT (lane 6), suggesting that the CCT binds to Cdc20's WD repeats. Analysis of C-terminal deletions suggested that the binding site was located within repeats 3–5 (lanes 1–4). Indeed, a fragment containing repeats 3–5 (residues 333–460) efficiently bound to the CCT (lane 9), whereas no or very weak interactions were observed for repeats 1–3 and 5–7 (lanes 8 and 10). A slightly smaller fragment (342–460) still conferred strong binding (lane 12), but further truncations drastically reduced binding. We conclude that the CCT binding site resides within a Cdc20 fragment of 118 residues. In a structural model of Cdc20's propeller, this fragment forms the blades III and IV followed by sequences from blade V, which pack against blade IV (Figure 6A). In contrast, only the N-terminal 130 residues of Cdc20 were dispensable for association with the APC/C whereas the WD repeats and the C-terminal region were essential (Figure 6B and data not shown). These data show that CCT and the APC/C recognize different structures within the Cdc20 molecule.

Mad2 only bound to Cdc20 fragments containing the previously defined Mad2 binding site in the N-terminal region (Hwang et al., 1998). Although binding of Mad2 to full-length Cdc20 required CCT activity, Mad2 also bound to Cdc20 fragments lacking the CCT binding region (Figure 6B, lanes 4 and 6). Accordingly, in extracts from *cct1-2* cells shifted to 37°C, Mad2 was associated with the N-terminal fragment but not with the full-length protein or a variant lacking the first 130 residues (Figure 6C). These data suggest that it is the presence of the WD propeller that renders binding of Mad2 to Cdc20 dependent on CCT function.

### Activation of the APC/C by Cdh1 Depends on CCT

We next asked whether Cdh1, the G1-specific activator of the APC/C, also required CCT function. As shown in Figure 7A, Cdh1 can bind to the CCT throughout the cell cycle because Myc18-Cdh1 was associated with Cct2-ha3 in extracts from growing cells, from elutriated G1 cells, from cells arrested in S phase, and from cells arrested in mitosis. This interaction was not detected with *cct1-2* mutant cells, demonstrating that it depends on a functional CCT complex (Figure 7B). Furthermore, Myc18-Cdh1 was released from the CCT in the presence of ATP but not in the presence of nonhydrolyzable ATP-analogs (Figure 7C). We conclude that Cdh1 shows the properties of a CCT substrate. We then investigated whether the CCT was required for the activity of the APC/C-Cdh1 holoenzyme in vivo. Inactivation of the APC/C in G1-arrested cells was shown to cause precocious accumulation of mitotic cyclins and entry into S phase (Irniger and Nasmyth, 1997). Indeed, *cct1-2* cells arrested in G1 with α factor and then shifted to 37°C accumulated Clb2 and initiated DNA replication (data not shown). However, it was possible that the *cct1-2* mutant cells accumulated Clb2 not because Cdh1 was defective but because they entered the cell cycle due to a defect in pheromone signaling. To address this possibility, we analyzed α factor-arrested wild-type, *cct1-2*, and *cdc16-123* strains all containing a *cdc28-4* mutation and expressing Clb2-ha3 from a weak, constitutive promoter. The *cdc28-4* mutation, which inactivates the Cdk1 kinase, ensured that all strains remained arrested in G1 at 37°C. As shown in Figure 7D, Clb2-ha3 accumulated in *cdc16-123 cdc28-4* and to a lesser extent in *cct1-2 cdc28-4* cells, but not in the *cdc28-4* control cells. These data demonstrate that the CCT is indeed required in G1-

(C) *Myc18-CDC20 CDC23-ha3* (+, Z450) and *Myc18-CDC20 CDC23* (−, Z446) cells were treated with 0.1 mM latrunculin B for 120 min (Lat B) or left untreated (Cyc). Left panel, Analysis of anti-HA immunoprecipitates. Right panel, staining of F-actin with rhodamine-phalloidin in *Myc18-CDC20 CDC23-ha3* cells.

(D) Strains of the indicated genotypes were grown at 25°C, shifted to 37°C for 120 min, and then mixed. Anti-HA immunoprecipitates were analyzed by immunoblotting with antibodies to HA and Cdc20. Strains: 1, Z651; 2, Z144 + Z446; 3, Z1085 + Z1109; 4, Z1111 + Z1088; 5, Z1113 + Z651; 6, Z1090 + Z651.

(E) Immunoblot analysis of anti-Myc immunoprecipitates prepared from wild-type and *cct1-2* strains containing *Myc9-CDC20* or *MAD1-myc9* grown at 25°C and shifted to 37°C for 120 min. Strains: 1, Z651; 2, Z2548; 3, Z1009; 4, Z2422; 5, Z2942; 6, Z2946.

(F) *BUB3-ha3* (+) and *BUB3* (−) strains containing *Myc18-BUB1* or *Myc18-CDC20* and *CCT1* or *cct1-2* were grown at 25°C, shifted to 37°C for 90 min, and processed for anti-HA immunoprecipitations. Strains: 1, Z651; 2, Z2211; 3, Z2262; 4, Z1725; 5, Z1812; 6, Z2258; 7, Z446.

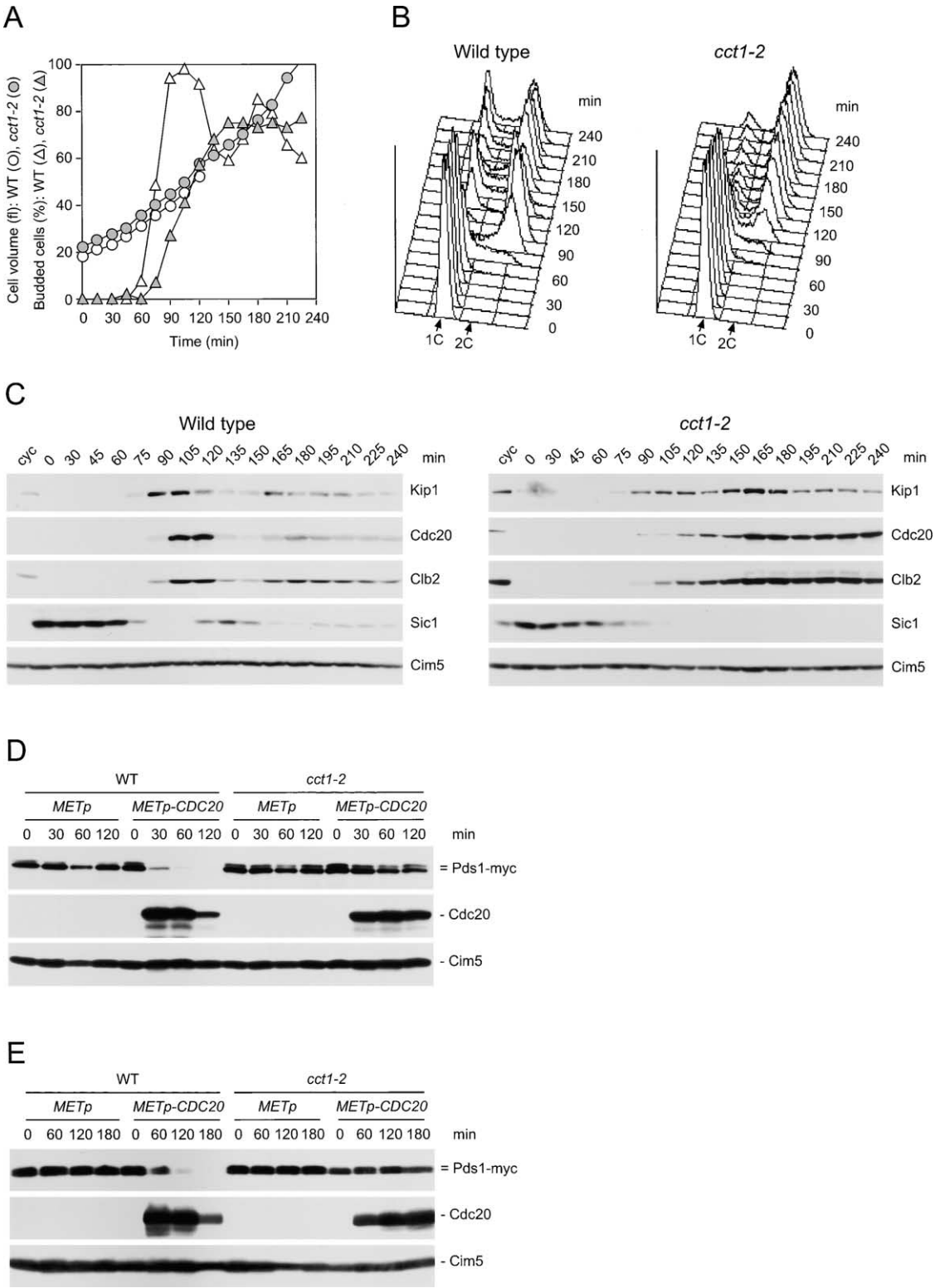


Figure 4. Analysis of CCT Function In Vivo

(A) Release at 37°C of elutriated G1 cells of wild-type (Z651, open symbols) and *cct1-2* (Z1323, filled symbols) strains. Samples were withdrawn every 15 min to measure the fraction of budded cells (triangles) and the mean cell volume (circles).

(B) Cellular DNA content.

(C) Immunoblot analysis of protein levels.

(D) *PDS1-myc18* wild-type and *PDS1-myc18 cct1-2* cells containing *CDC20* under the control of the *MET25* promoter (*METp-CDC20*, Z1226 and Z1271) or the *MET25* promoter alone (*METp*, Z1265 and Z1310) were grown at 24°C in medium containing methionine (*MET* promoter off), shifted to 37°C for 30 min, and transferred into medium lacking methionine at 37°C (*MET* promoter on). Samples taken at different times were analyzed by immunoblotting. Endogenous Cdc20 is only detectable on longer exposures.

(E) Strains were first arrested with hydroxyurea in methionine-containing medium at 24°C and then treated as in (D) using media containing hydroxyurea.

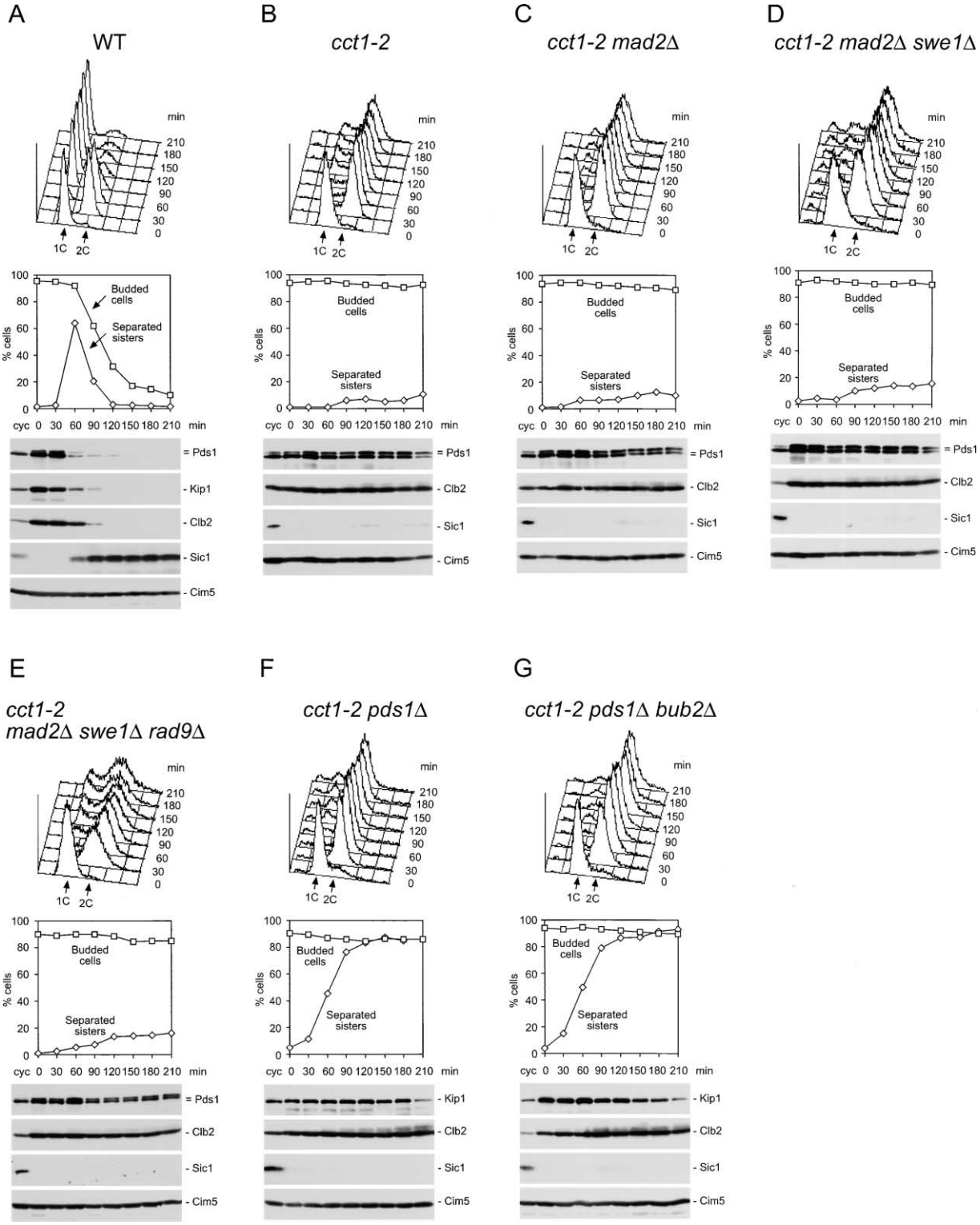


Figure 5. CCT Is Required for Entry into and Exit from Anaphase

Strains containing *PDS1-myc18* and a GFP-marked *URA3* locus were arrested at 23°C with hydroxyurea, shifted to 37°C for 30 min, washed, and then released at 37°C into medium lacking hydroxyurea and containing α factor. Sample were withdrawn at the indicated times to measure cellular DNA content (top panel), the fraction of budded cells, and of cells with separated sister chromatids (middle panel), and the level of proteins by immunoblotting (bottom panel). Strains: (A) Z1370, (B) Z1377, (C) Z1369, (D) Z1574, (E) Z2004, (F) Z1427, (G) Z1548.

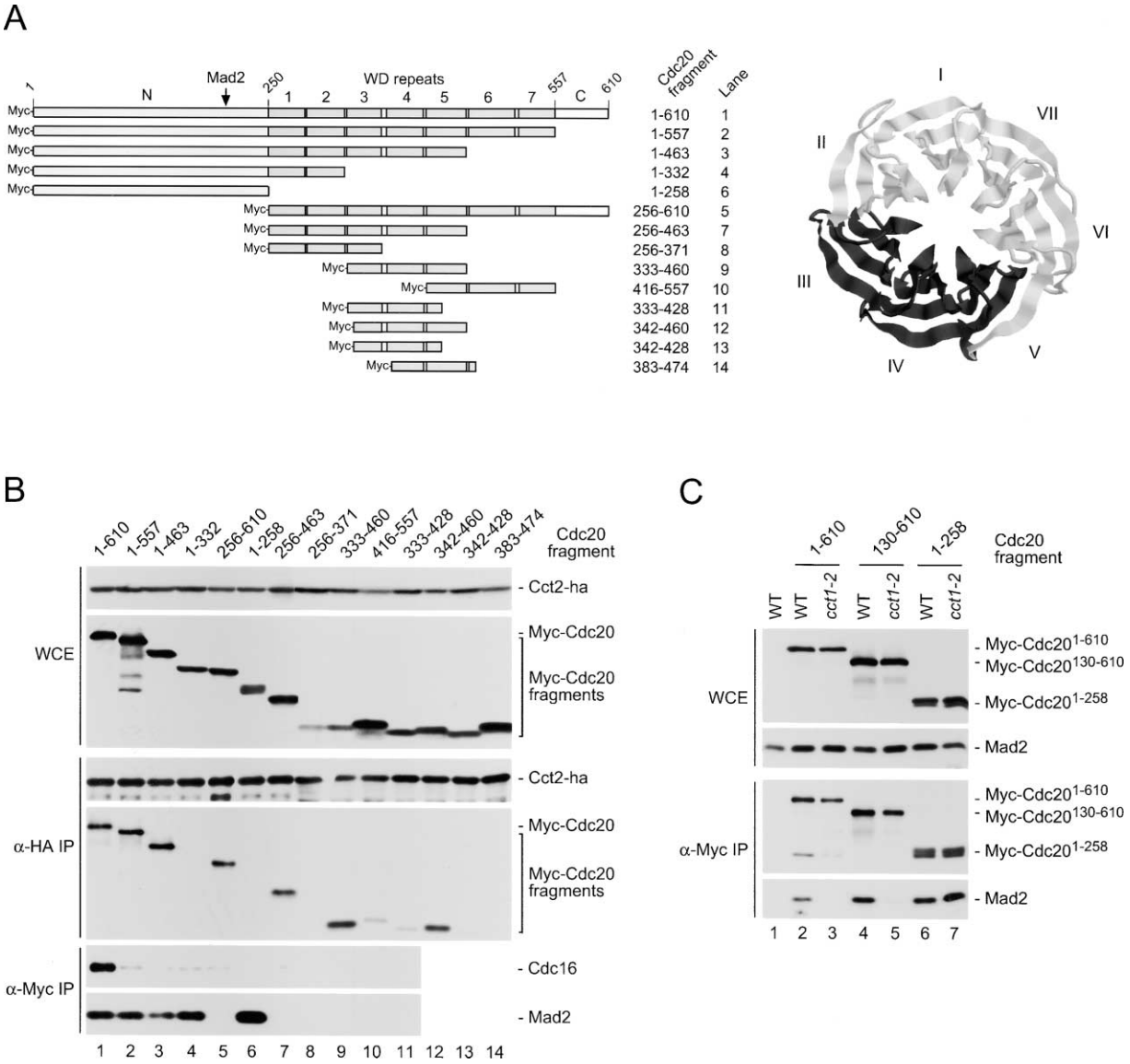


Figure 6. Identification of Cdc20 Sequences Recognized by the CCT

(A) Cdc20 domain structure and deletion constructs. Left panel, Cdc20 contains an N-terminal region harboring the Mad2 binding site, seven WD repeats, and a C-terminal region. Lane numbers refer to (B). Right panel, Cdc20's WD repeats were modeled onto the structure of β-tranducin (Sondek et al., 1996). Blades are numbered and the CCT binding site is shaded.

(B) Binding of Cdc20 fragments to the CCT, the APC/C, and Mad2. Cdc20 fragments tagged with Myc18 were expressed from the *GAL1* promoter for 90 min at 30°C in *CCT2-ha3* strains. Extracts, anti-HA, and anti-Myc immunoprecipitates were analyzed by immunoblotting. Strains: 1, Z1464; 2, Z1583; 3, Z1801; 4, Z1799; 5, Z1606; 6, Z1466; 7, Z1873; 8, Z1919; 9, Z1874; 10, Z1925; 11, Z2174; 12, Z2243; 13, Z2183; 14, Z2178.

(C) Binding of Mad2 to Cdc20 fragments in wild-type and *cct1-2* cells. Wild-type and *cct1-2* strains expressing Myc9-tagged Cdc20 fragments from the *CDC20* promoter were grown at 25°C, shifted to 37°C for 120 min, and processed for anti-Myc immunoprecipitations. Strains: 1, Z651; 2, Z1009; 3, Z2422; 4, Z2810; 5, Z2812; 6, Z2488; 7, Z2867.

arrested cells for the activity of APC/C-Cdh1 to prevent the precocious accumulation of mitotic cyclins. We conclude that both Cdc20 and Cdh1 require CCT to activate the APC/C.

## Discussion

The identification of natural substrates of the CCT is important to unravel the cellular functions of this chaperonin. In particular, the spectrum of physiological substrates and the mechanism of substrate recognition are poorly understood (Dunn et al., 2001). Initially, the CCT was thought to fold only actin and tubulin but the identification of other, noncytoskeletal, proteins requiring CCT for proper folding suggests that the chaperonin is important for a variety of cellular processes.

Here we provide evidence that the APC/C activator Cdc20 is a substrate of the CCT in budding yeast and

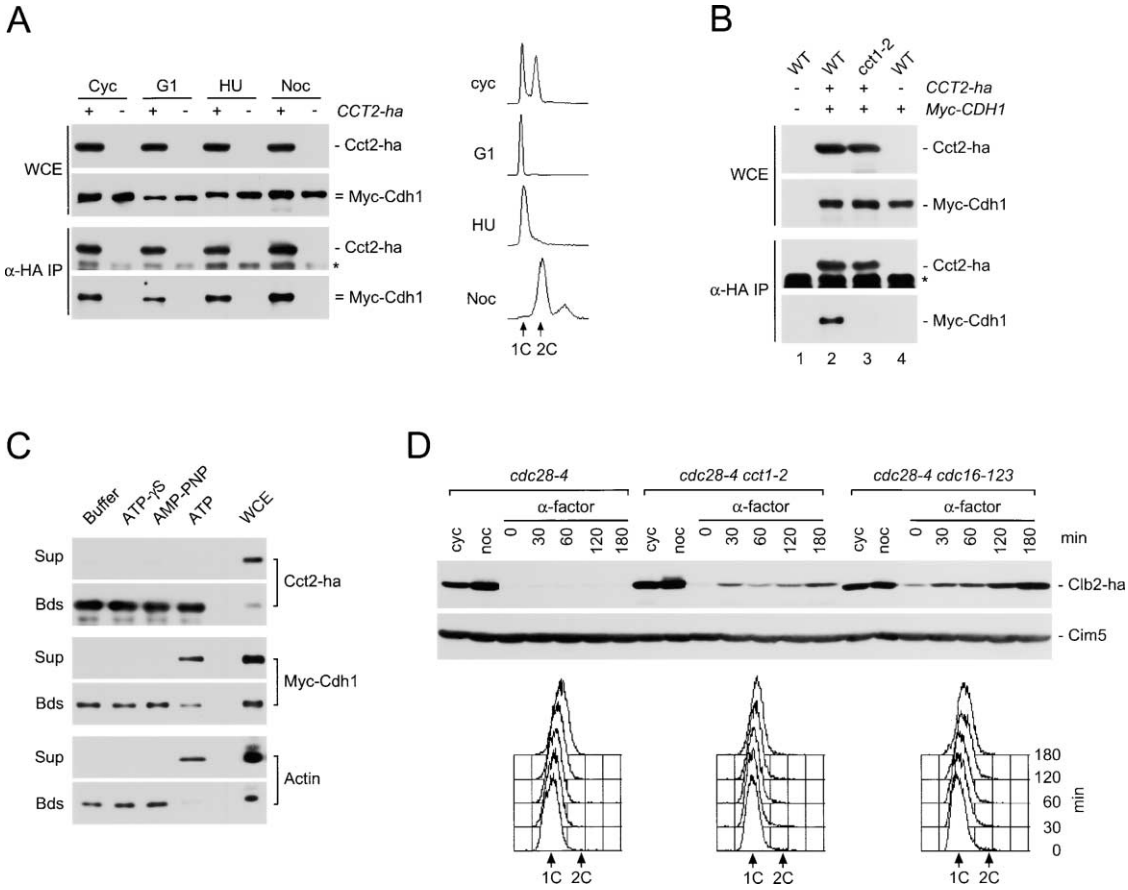


Figure 7. Characterization of the CCT-Cdh1 Interaction

(A) Growing cells (Cyc), elutriated G1 cells (G1), hydroxyurea-arrested cells (HU), and nocodazole-arrested cells (Noc) were obtained from *Myc18-CDH1 CCT2-ha3* (+, Z973) and *Myc18-CDH1* (−, Z483) strains. Left panel, immunoblot analysis of anti-HA immunoprecipitates. Right panel, cellular DNA content of *Myc18-CDH1 CCT2-ha3* cells.

(B) Strains containing tagged (+) or untagged (−) *CCT2* and *CDH1* and the indicated *CCT1* alleles were grown at 25°C, shifted to 37°C for 90 min, and processed for anti-HA immunoprecipitations. Strains: 1, Z651; 2, Z972; 3, Z1867; 4, Z484.

(C) Anti-HA immunoprecipitates from *CCT2-ha3 Myc18-CDH1 pep4Δ* cells (Z1914) were incubated for 20 min at 25°C with buffer, Mg/ATP, or the nonhydrolyzable analogs Mg/ATP-γS and Mg/AMP-PNP. Reactions were stopped, separated into supernatant (Sup) and beads (Bds) fractions, and analyzed by immunoplotting as in Figure 2.

(D) *MAT***a** *pep4Δ bar1Δ* strains expressing *CLB2-ha3* from the *S. pombe adh1* promoter and containing *cdc28-4* (Z2067), *cdc28-4 cct1-2* (Z2069), or *cdc28-4 cdc16-123* (Z2089) were grown at 25°C (cyc) and arrested in G1 with α factor. Strains were shifted to 37°C and samples were withdrawn at different times for immunoblot analysis (top panel) and to measure cellular DNA content (bottom panels). Strains were also arrested with nocodazole at 25°C and shifted to 37°C for 90 min (noc).

probably also in human cells. Cdc20 binds to the CCT in vivo and is released from the chaperonin upon hydrolysis of ATP. CCT is essential for Cdc20's ability to bind to the APC/C and to activate APC/C-dependent proteolysis. CCT was only required by Cdc20 but not by the APC/C to form the APC/C-Cdc20 holoenzyme. The APC/C from *cct1-2* mutant cells could still bind to exogenous Cdc20, excluding the possibility that the CCT is required for the integrity of the APC/C or a modification essential for binding to Cdc20. As predicted by these results, CCT was required in vivo for Cdc20-dependent cell cycle events such as sister chromatid separation and exit from mitosis even in cells lacking checkpoint pathways. CCT was also required for the function of the Cdc20-related protein Cdh1, which activates the APC/C during G1.

How does the CCT convert the APC/C activators into functional molecules and when does this reaction occur in the lifetime of these proteins? WD repeats fold into a β propeller whose blades consist of a four-stranded β sheet. The propeller is stabilized by many hydrophobic interactions, which can only be buried in the protein upon completion of translation because the propeller is closed by interactions involving the first and the last repeat (Smith et al., 1999). Folding of Cdc20's propeller might require the exclusive environment of CCT's central cavity to prevent nonnative interactions of the nascent WD repeats. Indeed, CCT binds to WD repeats of Cdc20, and the dimensions of a WD propeller are compatible with folding inside the cavity. The idea that WD proteins are particularly dependent on CCT is supported by a recent study in yeast in which 600 epitope-tagged pro-

teins, including 45 WD proteins, were immunopurified to identify multisubunit complexes (Ho et al., 2002). A total of 24 proteins were found to be associated with 3 or more CCT subunits and 16 of those contained WD repeats.

Our data also suggest that certain WD repeat proteins can fold without CCT's assistance. Cdc4 and Bub3 did not interact with the CCT, and both proteins were functional in *cct1-2* mutant cells at 37°C. Currently, we do not understand what distinguishes WD proteins requiring CCT from those that do not. One possibility is that the CCT is required for the proper interaction between the propeller and another domain such as the N-terminal regions of Cdc20 and Cdh1. Digestion of human Cdc20 with chymotrypsin produces two fragments, the N-terminal region and the propeller, indicating that Cdc20 indeed behaves as a two-domain protein (Tang et al., 2001). The integrity of both domains is required for binding to the APC/C. A "domain model" could explain why binding of Mad2 to full-length Cdc20 required CCT activity, whereas binding to the N-terminal fragment by itself did not. In *cct1-2* mutant cells, a nonnative interaction between the N-terminal region and the propeller might block access of Mad2 to its binding site. Accordingly, Mad2 from *cct1-2* cells could still bind to Mad1, which possesses a Mad2 binding site similar to that in Cdc20 but lacks WD repeats (Luo et al., 2002; Sironi et al., 2002). CCT could arrange the domains of newly synthesized Cdc20 but could also function posttranslationally. Binding of Cdc20 to APC/C, APC/C substrates, or checkpoint proteins may involve conformational changes requiring the CCT.

The chaperone complex GimC/prefoldin binds to nascent chains of actin and tubulin and delivers them to the CCT (Hansen et al., 1999). We failed to detect any interaction of Cdc20 with GimC/prefoldin in wild-type and *cct1-2* mutant extracts. Furthermore, binding of Cdc20 to the APC/C was normal in different *gim* mutants, suggesting that the chaperone is not required for Cdc20 function. CCT might fold certain substrates without involving GimC/prefoldin.

A recent analysis of CCT-associated proteins from human cells detected at least 70 polypeptides in addition to actin and tubulin (Thulasiraman et al., 1999). However, only a few noncytoskeletal substrates have been identified, including G$\alpha$-tranducin (Farr et al., 1997), cyclin E (Won et al., 1998), von Hippel-Lindau tumor suppressor protein (VHL) (Feldman et al., 1999), histone deacetylase 3 (Guenther et al., 2002), and, as shown here, the APC/C activators. It is unclear how the CCT recognizes a distinct set of substrates displaying such structural diversity. Whereas the bacterial chaperonin GroEL interacts with unfolded polypeptides through nonspecific, hydrophobic interactions, CCT is thought to use a specific mechanism. Cryoelectron microscopy of CCT bound to actin and tubulin suggested that individual subunits recognize defined motifs within the substrate (Llorca et al., 2000). The CCT binding sites of VHL (Feldman et al., 1999) and Cdc20 consist of $\beta$ sheets, but whether this structure is generally important for substrate recognition remains to be investigated. The structures of different WD propellers and of different blades within one propeller are remarkably similar, yet CCT is able to distinguish them, supporting the idea of a specific recognition mechanism. A detailed analysis of different WD proteins might help to understand how the chaperonin recognizes its substrates.

## Experimental Procedures

### Strains and Growth Conditions

Yeast strains were derivatives of W303 (K699). Strains were grown in YPA medium (Sherman, 1991) containing 2% glucose (YPAD) or 2% raffinose (YPRaf). To induce the *GAL1* promoter, 2% galactose was added to cultures grown in YPRaf medium. To induce the *MET25* promoter, strains grown in YPRaf medium containing methionine (5 mM) were washed by filtration with eight culture volumes of SC medium lacking methionine (Sherman, 1991) and inoculated into the same medium. Cells were arrested in S phase with hydroxyurea (0.1 M) and in mitosis with nocodazole (15 $\mu$g/ml). For arrest/release experiments, strains arrested with hydroxyurea in YPRaf medium were washed by filtration with 20 culture volumes of YPAD medium ($\leq$10 min) and released into YPAD medium. $\alpha$ factor (0.5 $\mu$g/ml) was used to arrest *MAT***a** *bar1*$\Delta$ strains in G1. Small G1 cells were isolated by centrifugal elutriation from cultures grown in YPRaf medium at 25°C and released into YPAD medium at 37°C.

### Plasmid and Strain Constructions

Standard techniques were used to manipulate DNA and to construct yeast strains. PCR-generated cassettes were used for gene replacement and C-terminal epitope tagging (Knop et al., 1999; Wach et al., 1997). *CCT1-ha3* and *CCT2-ha3* strains grew like wild-type strains at different temperatures. *CCT1-ha3 cct4-1*, *CCT2-ha3 cct1-2*, and *CCT2-ha3 cct4-1* strains grew well at 25°C, whereas double ts mutants were inviable. The *cct4-1/anc2-1* mutation (Vinh and Drubin, 1994) was introduced into W303 through four backcrosses. To construct *cct1-2* mutants and control strains, *URA3* plasmids containing the *cct1-2/tcp1-2* allele (Ursic et al., 1994) or the wild-type gene were integrated into one *ura3* locus of a *cct1*$\Delta$*::HIS3/CCT1* diploid strain followed by tetrad dissection. The *cct1*$\Delta$*::HIS3 ura3::cct1-2::URA3* and the control strains behaved like *cct1-2* and wild-type strains, respectively. The *cct1-2* mutation was introduced into the *CCT1* locus by pop-in/pop-out replacement (Rothstein, 1991). Plasmids expressing *CDC20* from the *MET25* promoter were integrated at the *trp1* locus. For Figure 6B, plasmids expressing *Myc18-CDC20* fragments from the *GAL1* promoter were integrated into the *leu2* loci of wild-type and *CCT2-ha3* strains. Fragments were amplified from *Myc18-CDC20* plasmids described in Shirayama et al. (1998). For Figure 6C, plasmids containing *Myc9-CDC20* fragments expressed from the *CDC20* promoter were integrated into the *leu2* loci of wild-type and *cct1-2* strains.

### Antibodies

Actin, human Cdc27, HA epitope, and Myc epitope were detected with the mouse monoclonal antibodies C4 (ICN), AF3.1 (Santa Cruz), 12CA5, and 9E10, respectively. Human Cct$\alpha$/Cct1 and Cct$\delta$/Cct4 were detected with the rat monoclonal antibodies 84a (Stressgene) and 8g (provided by K. Willison), respectively. Rabbit antibodies to human Cdc20 (H-175; Santa Cruz) and human chTOG (provided by A. Hyman) were used for immunoprecipitations. Rabbit antibodies to the yeast proteins $\beta$-tubulin (W. Seufert), Cdc16 and Cdc27 (P. Hieter), Clb2 (D. Kellog), Cim5 (C. Mann), Kip1 (A. Hyman), Mad2 (K. Hardwig), and Sic1 (M. Tyers) were gifts from the indicated researchers. To raise antibodies, His6-tagged Apc2 (full-length), Cct1 (residues 268–486), and Cdc20 (470–610) were expressed in *E. coli* and purified on Ni-NTA resign under denaturing conditions. Proteins were electro-eluted from preparative SDS gels and used to immunize rabbits at Eurogentec (Herstal, Belgium).

### Analysis of Proteins

Glycerol density gradient centrifugations and immunoprecipitations from $^{35}$S-labeled extracts were performed as described (Zachariae et al., 1996). For protein identification, anti-Myc immunoprecipitations were prepared from $2.3 \times 10^{10}$ *PDS1-myc18 pep4*$\Delta$ (control) and *Myc18-CDC20 pep4*$\Delta$ cells (Zachariae et al., 1998). Corresponding bands from the Myc18-Cdc20 and the control sample were excised from a silver-stained gel and analyzed by nano-electrospray tandem

mass spectrometric sequencing (Shevchenko et al., 1996). For immunoprecipitation-immunoblotting experiments, extracts were prepared from $2 \times 10^6$ cells in 0.4 ml of buffer B70 (Zachariae et al., 1998) (numbers indicate millimolar K acetate). Cleared extracts (0.35 ml, 4 mg) were incubated for 60 min with antibodies, which were captured with 40 μl of protein A-Sepharose for 60 min. Beads were washed with the buffers B70 plus BSA (1 mg/ml), B70, B150, B200, and B70 followed by immunoblot analysis. CCT's specificity was analyzed by probing anti-HA immunoprecipitates from *CCT2-ha3* cells with antibodies to Adh1, Apc2, Cct1, Cdc11, Cdc16, Cdc20, Cdc28, Cim3, Cim5, Clb2, Ctf19, Kip1, Mad2, Mif2, Ndc10, Ndc80, Nop1, PFK, Sec4, Sso2, Stu2, Swi6, Tub2, and Ubc9. Only Cct1, Cdc20, and Tub2 were associated with Cct2-ha3. To release CCT substrates, anti-HA immunoprecipitates from *CCT1-ha3 Myc9-CDC20* or *CCT2-ha3 Myc18-CDH1* cells were further washed for 15 min at 25°C with buffer B70 plus 0.2% NP40. Reactions containing 40 μl beads in B70 buffer were supplemented with Mg/ATP (2 mM), incubated at 25°C, and stopped with EDTA (15 mM). After centrifugation, the supernatants were filtered through empty spin columns, and the beads were washed three times with buffer B70. Supernatants and bound proteins were analyzed by immunoblotting. HeLa cells were scraped from the plates in PBS and lysed in buffer B100 plus 0.8% NP40. Cleared extracts (0.4 ml, 6 mg) were subjected to immunoprecipitations, and beads were washed four times with buffer B100 containing 0.5% NP40.

### Other Techniques

The peak cell volume of nonfixed cells was measured with a CASY1 Cell Counter Analyser (Schaerfe System, Reutlingen, Germany). Observation of sister chromatids and flow cytometric analysis of cellular DNA content were performed as described (Michaelis et al., 1997).

### Acknowledgments

We are grateful to K. Nasmyth, in whose laboratory the first experiment was performed, for generously providing many yeast strains and plasmids. We thank B. Habermann for cell culture and bioinformatics, R. Deshaies, G. Drubin, A. Horwich, S. Piatti, and D. Ursic for yeast strains and plasmids, and K. Hardwick, P. Hieter, A. Hyman, C. Mann, E. Schiebel, W. Seufert, K. Siegers, M. Tyers, and K. Willison for antibodies. We also thank E. Tanaka and M. Schwickart for critically reading the manuscript. This work was supported by the Max Planck Gesellschaft and a grant from the Human Frontier Science Program Organization (RG0364/1999-M) to W.Z.

Received: January 1, 2003
Revised: April 11, 2003
Accepted: April 25, 2003
Published: July 24, 2003

### References

Amon, A., Tyers, M., Futcher, B., and Nasmyth, K. (1993). Mechanisms that help the yeast cell cycle clock tick: G2 cyclins transcriptionally activate G2 cyclins and repress G1 cyclins. Cell *74*, 993–1007.

Burke, D.J. (2000). Complexity in the spindle checkpoint. Curr. Opin. Genet. Dev. *10*, 26–31.

Ciosk, R., Zachariae, W., Michaelis, C., Shevchenko, A., Mann, M., and Nasmyth, K. (1998). An ESP1/PDS1 complex regulates loss of sister chromatid cohesion at the metaphase to anaphase transition in yeast. Cell *93*, 1067–1076.

Dunn, A.Y., Melville, M.W., and Frydman, J. (2001). Review: cellular substrates of the eukaryotic chaperonin TRiC/CCT. J. Struct. Biol. *135*, 176–184.

Farr, G.W., Scharl, E.C., Schumacher, R.J., Sondek, S., and Horwich, A.L. (1997). Chaperonin-mediated folding in the eukaryotic cytosol proceeds through rounds of release of native and nonnative forms. Cell *89*, 927–937.

Feldman, D.E., Thulasiraman, V., Ferreyra, R.G., and Frydman, J. (1999). Formation of the VHL-elongin BC tumor suppressor complex is mediated by the chaperonin TRiC. Mol. Cell *4*, 1051–1061.

Glotzer, M., Murray, A.W., and Kirschner, M.W. (1991). Cyclin is degraded by the ubiquitin pathway. Nature *349*, 132–138.

Gordon, D.M., and Roof, D.M. (2001). Degradation of the kinesin Kip1p at anaphase onset is mediated by the anaphase-promoting complex and Cdc20p. Proc. Natl. Acad. Sci. USA *98*, 12515–12520.

Guenther, M.G., Yu, J., Kao, G.D., Yen, T.J., and Lazar, M.A. (2002). Assembly of the SMRT-histone deacetylase 3 repression complex requires the TCP-1 ring complex. Genes Dev. *16*, 3130–3135.

Gutsche, I., Essen, L.O., and Baumeister, W. (1999). Group II chaperonins: new TRiC(k)s and turns of a protein folding machine. J. Mol. Biol. *293*, 295–312.

Hansen, W.J., Cowan, N.J., and Welch, W.J. (1999). Prefoldin-nascent chain complexes in the folding of cytoskeletal proteins. J. Cell Biol. *145*, 265–277.

Ho, Y., Gruhler, A., Heilbut, A., Bader, G.D., Moore, L., Adams, S.L., Millar, A., Taylor, P., Bennett, K., Boutilier, K., et al. (2002). Systematic identification of protein complexes in Saccharomyces cerevisiae by mass spectrometry. Nature *415*, 180–183.

Hwang, L.H., Lau, L.F., Smith, D.L., Mistrot, C.A., Hardwick, K.G., Hwang, E.S., Amon, A., and Murray, A.W. (1998). Budding yeast Cdc20: a target of the spindle checkpoint. Science *279*, 1041–1044.

Irniger, S., and Nasmyth, K. (1997). The anaphase-promoting complex is required in G1 arrested yeast cells to inhibit B-type cyclin accumulation and to prevent uncontrolled entry into S-phase. J. Cell Sci. *110*, 1523–1531.

Knop, M., Siegers, K., Pereira, G., Zachariae, W., Winsor, B., Nasmyth, K., and Schiebel, E. (1999). Epitope tagging of yeast genes using a PCR-based strategy: more tags and improved practical routines. Yeast *15*, 963–972.

Lew, D.J. (2000). Cell-cycle checkpoints that ensure coordination between nuclear and cytoplasmic events in Saccharomyces cerevisiae. Curr. Opin. Genet. Dev. *10*, 47–53.

Llorca, O., Martin-Benito, J., Ritco-Vonsovici, M., Grantham, J., Hynes, G.M., Willison, K.R., Carrascosa, J.L., and Valpuesta, J.M. (2000). Eukaryotic chaperonin CCT stabilizes actin and tubulin folding intermediates in open quasi-native conformations. EMBO J. *19*, 5971–5979.

Luo, X., Tang, Z., Rizo, J., and Yu, H. (2002). The Mad2 spindle checkpoint protein undergoes similar major conformational changes upon binding to either Mad1 or Cdc20. Mol. Cell *9*, 59–71.

Michaelis, C., Ciosk, R., and Nasmyth, K. (1997). Cohesins: chromosomal proteins that prevent premature separation of sister chromatids. Cell *91*, 35–45.

Musacchio, A., and Hardwick, K.G. (2002). The spindle checkpoint: structural insight into dynamic signalling. Nat. Rev. Mol. Cell Biol. *3*, 731–741.

Nasmyth, K., Peters, J.M., and Uhlmann, F. (2000). Splitting the chromosome: cutting the ties that bind sister chromatids. Science *288*, 1379–1385.

Peters, J.M. (2002). The anaphase-promoting complex: proteolysis in mitosis and beyond. Mol. Cell *9*, 931–943.

Prinz, S., Hwang, E.S., Visintin, R., and Amon, A. (1998). The regulation of Cdc20 proteolysis reveals a role for APC components Cdc23 and Cdc27 during S phase and early mitosis. Curr. Biol. *8*, 750–760.

Rothstein, R. (1991). Targeting, disruption, replacement, and allele rescue: integrative DNA transformation in yeast. Methods Enzymol. *194*, 281–301.

Sherman, F. (1991). Getting started with yeast. Methods Enzymol. *194*, 3–21.

Shevchenko, A., Jensen, O.N., Podtelejnikov, A.V., Sagliocco, F., Wilm, M., Vorm, O., Mortensen, P., Shevchenko, A., Boucherie, H., and Mann, M. (1996). Linking genome and proteome by mass spectrometry: large-scale identification of yeast proteins from two dimensional gels. Proc. Natl. Acad. Sci. USA *93*, 14440–14445.

Shirayama, M., Zachariae, W., Ciosk, R., and Nasmyth, K. (1998). The Polo-like kinase Cdc5p and the WD-repeat protein Cdc20p/fizzy

are regulators and substrates of the anaphase promoting complex in Saccharomyces cerevisiae. EMBO J. *17*, 1336–1349.

Sironi, L., Mapelli, M., Knapp, S., De Antoni, A., Jeang, K.-T., and Musacchio, A. (2002). Crystal structure of the tetrameric Mad1-Mad2 core complex: implications of a "safety belt" binding mechanism for the spindle checkpoint. EMBO J. *21*, 2496–2506.

Smith, T.F., Gaitatzes, C., Saxena, K., and Neer, E.J. (1999). The WD repeat: a common architecture for diverse functions. Trends Biochem. Sci. *24*, 181–185.

Sondek, J., Bohm, A., Lambright, D.G., Hamm, H.E., and Sigler, P.B. (1996). Crystal structure of a G-protein beta gamma dimer at 2.1 Å resolution. Nature *379*, 369–374.

Sternlicht, H., Farr, G.W., Sternlicht, M.L., Driscoll, J.K., Willison, K., and Yaffe, M.B. (1993). The t-complex polypeptide 1 complex is a chaperonin for tubulin and actin in vivo. Proc. Natl. Acad. Sci. USA *90*, 9422–9426.

Stoldt, V., Rademacher, F., Kehren, V., Ernst, J.F., Pearce, D.A., and Sherman, F. (1996). Review: the Cct eukaryotic chaperonin subunits of Saccharomyces cerevisiae and other yeasts. Yeast *12*, 523–529.

Tang, Z., Bharadwaj, R., Li, B., and Yu, H. (2001). Mad2-Independent inhibition of APCCdc20 by the mitotic checkpoint protein BubR1. Dev. Cell *1*, 227–237.

Thulasiraman, V., Yang, C.F., and Frydman, J. (1999). In vivo newly translated polypeptides are sequestered in a protected folding environment. EMBO J. *18*, 85–95.

Ursic, D., Sedbrook, J.C., Himmel, K.L., and Culbertson, M.R. (1994). The essential yeast Tcp1 protein affects actin and microtubules. Mol. Biol. Cell *5*, 1065–1080.

Vinh, D.B., and Drubin, D.G. (1994). A yeast TCP-1-like protein is required for actin function in vivo. Proc. Natl. Acad. Sci. USA *91*, 9116–9120.

Visintin, R., Prinz, S., and Amon, A. (1997). CDC20 and CDH1: a family of substrate-specific activators of APC-dependent proteolysis. Science *278*, 460–463.

Vodermaier, H.C. (2001). Cell cycle: Waiters serving the Destruction machinery. Curr. Biol. *11*, R834–R837.

Wach, A., Brachat, A., Alberti-Segui, C., Rebischung, C., and Philippsen, P. (1997). Heterologous HIS3 marker and GFP reporter modules for PCR-targeting in Saccharomyces cerevisiae. Yeast *13*, 1065–1075.

Wang, H., Liu, D., Wang, Y., Qin, J., and Elledge, S.J. (2001). Pds1 phosphorylation in response to DNA damage is essential for its DNA damage checkpoint function. Genes Dev. *15*, 1361–1372.

Won, K.A., Schumacher, R.J., Farr, G.W., Horwich, A.L., and Reed, S.I. (1998). Maturation of human cyclin E requires the function of eukaryotic chaperonin CCT. Mol. Cell. Biol. *18*, 7584–7589.

Zachariae, W., and Nasmyth, K. (1999). Whose end is destruction: cell division and the anaphase-promoting complex. Genes Dev. *13*, 2039–2058.

Zachariae, W., Shin, T.H., Galova, M., Obermaier, B., and Nasmyth, K. (1996). Identification of subunits of the anaphase-promoting complex of Saccharomyces cerevisiae. Science *274*, 1201–1204.

Zachariae, W., Shevchenko, A., Andrews, P.D., Ciosk, R., Galova, M., Stark, M.J., Mann, M., and Nasmyth, K. (1998). Mass spectrometric analysis of the anaphase-promoting complex from yeast: identification of a subunit related to cullins. Science *279*, 1216–1219.